

# ĆUK CONVERTER CONTROL WITH A ROBUST INTEGRAL SWITCHING CONTROLLER

Günyaz ABLAY

Department of Electrical-Electronics Engineering, Abdullah Gül University, Kayseri, Turkey  
gunyaz.ablay@agu.edu.tr

**Abstract:** A robust control strategy for constant voltage reference tracking control of the Ćuk converters is presented in this study. The Ćuk converter can find many application places in industrial systems, but its topology has a non-minimum phase uncontrollable nonlinear dynamics, which poses problem in a low cost and high performance control design specifically under load/supply variations. An integral switching controller is designed to achieve robust operating conditions. The state averaging method and variable structure system theory are used in the design and analysis of the controller. The performance of the controlled Ćuk converter is evaluated via numerical simulations and circuit realizations to show the validity, feasibility and robustness of the controller.

**Key words:** Ćuk converter, dc-dc converters, switching control, tracking control.

## 1. Introduction

The Ćuk converter comprises minimum number of circuit elements and is one of the most significant nonlinear dc/dc switching power supply for industrial systems. Ćuk converters are utilized in many applications including power processing units, motor drive systems, automotive display systems, positive to negative conversion, power factor corrections, solar photovoltaic energy systems, LCD bias and MR Head bias [1]–[5]. The Ćuk converter has an inverting output voltage that can operate both above and below the source voltage. The Ćuk converter is a fourth-order non-minimum phase nonlinear system and it is difficult to stabilize this converter due to the uncontrolled and undamped resonance of the LC pair. Thus, design of an effective controller is critical for stabilization of the converter and for desirable control performances.

The Ćuk converter control techniques are predominantly based on the pulse-width modulation controllers in literature. The fixed-frequency PWM

based controllers utilize the current mode control to tackle with the stabilization problem of the converter. The control methods that have been applied to Ćuk converters include one-cycle control [6], [7], passivity-based control [8], model predictive control [9], [10], fuzzy logic based control [11], neural networks based control [12], state feedback control [13], nonlinear carrier control [14], [15], cascaded controllers [16]–[18] and sliding mode control [19], [20]. While good transient and steady-state control performances have been reported with these approaches, most of these methods require a full state feedback and complex control structures. The one-cycle control, an integrator reset based pulsed nonlinear method, offers a simple control structure, but the method is not robust against load variations and non-idealities of the components of the Ćuk converter.

This work proposes a robust switching integral control strategy for low-cost solutions and robust tracking control of Ćuk converters. It is shown in the literature that the Ćuk converter exhibits a non-minimum phase nonlinear dynamics and for this reason the traditional converter control methods are not able to provide desirable control performances. The most promising control strategy studied in the literature is the variable structure control with sliding modes [20], [21]. Since the Ćuk converter is a variable structure system, a wide range operating conditions with satisfactory performances can be accomplished with an appropriate variable structure control method. However, most of the sliding mode based controllers are designed with indirect current mode control which is not robust enough against load variations, or full state feedback control which is not cost effective to implement in practice. For these reasons, a simple and robust switching controller is designed and implemented in this work for providing a fast dynamic

response, a simple and cost effective control circuit and robustness in the presence of load and supply variations.

## 2. Control Design For Ćuk Converters

The Ćuk converter is a switching power converter providing a negative regulated output voltage which is either greater than or less than the input supply voltage. The Ćuk converter topology requires two inductors (usually coupled inductors), two capacitors, a switch and a diode. The circuit diagram of the Ćuk converter is shown in Fig. 1.

The inductors  $L_1$  and  $L_2$  convert the input voltage source into a current source and the capacitors  $C_1$  and  $C_2$  are used as energy storage elements. The switches of the converter work in a complementary fashion, namely, when the switching transistor is in the conducting mode then the diode is inversely polarized and vice-versa. The converter is difficult to stabilize, and often a complex control circuitry is required to make the converter operate appropriately. However, the control complexity increases the cost and slows down the dynamic response of the converter.

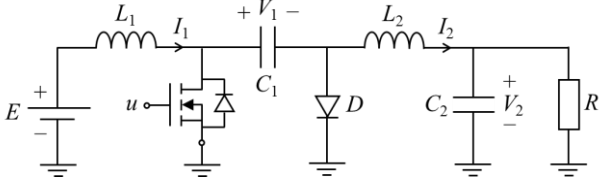


Fig. 1. The circuit diagram of the Ćuk converter.

Assuming that the parasitic elements, switch delays, switch voltage drops and auxiliary networks may be neglected. Then by considering the circuit structures within a switching period, i.e., off-state with  $u = 0$  and on-state with  $u = 1$ , a fourth-order nonlinear model is obtained for the Ćuk converter as:

$$\begin{aligned} L_1 \dot{I}_1 &= -(1-u)V_1 + E \\ C_1 \dot{V}_1 &= (1-u)I_1 + uI_2 \\ L_2 \dot{I}_2 &= -uV_1 - V_2 \\ C_2 \dot{V}_2 &= I_2 - V_2 / R \end{aligned} \quad (1)$$

where  $I_{1,2}$  and  $V_{1,2}$  represent inductor currents and capacitor voltages, the control signal  $u$  takes only discrete values,  $u \in \{0,1\}$ ,  $L_{1,2}$  and  $C_{1,2}$  indicate inductances and capacitances, and  $R$  represents the load resistance.

The control objective is to keep the output voltage constant during the tracking a reference voltage  $V_d < 0$ . That is, in the steady-state regime, the converter

output voltage must stay on the desired operating point. For a constant voltage reference  $\bar{V}_2 = V_d$ , the operating point of the Ćuk converter is obtained from (1) as

$$\bar{I}_1 = V_d^2 / RE, \bar{V}_1 = E - V_d, \bar{I}_2 = V_d / R, \bar{u} = V_d / (V_d - E) \quad (2)$$

where  $\bar{u}$  is the average control value during the steady-state. It can be shown from the linearization based analyses that the Ćuk converter is a fourth order non-minimum phase nonlinear system.

To meet the control goals (stabilization and reference tracking) of the Ćuk converter, a smooth switching manifold based switch-mode controller is a good candidate, because a variable structure controller with one switch can directly be applied for controlling the converter without making any modifications. This implies that a variable structure controller can ease the practical realizations. By considering the Ćuk converter dynamics defined by (1), a switching controller is proposed as

$$u = \begin{cases} 1, & \text{if } \rho(t) > 0 \\ 0, & \text{if } \rho(t) < 0 \end{cases} \quad (3)$$

$$\rho(t) = \varphi \int_0^t [V_d - V_2(\tau)] d\tau - I_1(t) \quad (4)$$

where  $V_d$  is a negative valued reference voltage, the control gain  $\varphi < 0$ , and  $\rho(t)$  is a switching manifold. When the time derivative of the switching manifold is zero,  $\dot{\rho}(t) = 0$ , the corresponding average control signal can be calculated as

$$u_{ave} = [V_1 - E + \varphi L_1 (V_d - V_2)] / V_1 \quad (5)$$

If the system operation does not reach saturating conditions, the average control ensures

$$0 < u_{ave} < 1 \quad (6)$$

with

$$\begin{aligned} V_1 - E + \varphi L_1 (V_d - V_2) &> 0 \\ E - \varphi L_1 (V_d - V_2) &> 0 \end{aligned} \quad (7)$$

Now, let us first analyze the system under the average control (5). The corresponding ideal system dynamics or zero dynamics can be written as

$$\begin{aligned} L_1 \dot{I}_1 &= \varphi L_1 (V_d - V_2) \\ C_1 \dot{V}_1 &= [E - \varphi L_1 (V_d - V_2)] [I_1 - I_2] / V_1 + I_2 \\ L_2 \dot{I}_2 &= -V_1 - V_2 - \varphi L_1 (V_d - V_2) + E \\ C_2 \dot{V}_2 &= I_2 - V_2 / R \end{aligned} \quad (8)$$

The nonlinear zero dynamics has the same operating point with (2). Since the equation (8) is nonlinear, the stability of the zero dynamics can be analyzed via linearizing the system around the operating point. The resulting linearized zero dynamics can be written as

$$\begin{aligned}
L_1 \dot{I}_1 &= \varphi L_1 (V_d - V_2) \\
C_1 \dot{V}_1 &= \frac{E}{E - V_d} I_1 + \frac{V_d}{R(E - V_d)} V_1 - \frac{V_d}{E - V_d} I_2 + \frac{\varphi L_1 V_d}{RE} (V_d - V_2) \\
L_2 \dot{I}_2 &= -V_1 - V_2 - \varphi L_1 (V_d - V_2) + E \\
C_2 \dot{V}_2 &= I_2 - V_2 / R
\end{aligned} \tag{9}$$

The eigenvalues of the system are calculated from  $\det(\lambda I - A) = 0$ , and it can be shown that the zero dynamics for the given operating point can always be made asymptotically stable for suitable converter parameters.

Next, we need to analyze the Ćuk converter dynamics under the switching controller (3) and (4). For a positive definite Lyapunov function,  $V = \rho^2/2 > 0$ , closed-loop stability is ensured if the time derivative of this function is negative definite,  $\dot{V} = \rho \dot{\rho} < 0$ . From (4), for a constant reference,  $V_d$ , the time derivative of the switching manifold can be written as

$$\dot{\rho} = [(1-u)V_1 - E] / L_1 + \varphi(V_d - V_2) \tag{10}$$

From (3), if  $\rho > 0$  and  $u = 1$ , then  $\dot{\rho} = \varphi(V_d - V_2) - E/L_1 < 0$  due to the condition (7) and  $\rho \dot{\rho} < 0$ . If  $\rho < 0$  and  $u = 0$ , then  $\dot{\rho} = \varphi(V_d - V_2) + (V_1 - E)/L_1 > 0$  due to the condition (7) and  $\rho \dot{\rho} < 0$ . Hence, the Ćuk converter under the proposed switching controller has stable dynamics.

### 3. Circuit Realizations and Results

#### A. Numerical Assessment of the Controller

The proposed controller design is first tested with MATLAB based numerical simulations. The converter is designed with  $L_1 = L_2 = 22\mu\text{H}$ ,  $C_1 = 2.2\mu\text{F}$ ,  $C_2 = 22\mu\text{F}$  (due to (11)), a supply voltage of  $E = 12\text{V}$  and a load resistance of  $R = 10\Omega$ . The control gain is selected as  $\varphi = -1000$ . The switching frequency of the PWM comparator is selected as  $f_s = 300\text{kHz}$ . Based on the linearized small signal model of the controlled Ćuk converter, the numerical frequency response (Bode diagram) from input to inductor current ( $I_1$ ) is given in Fig. 2, where a first-order system response is seen. In addition, when output capacitor voltage ( $V_2$ ) is taken as output, the controlled system exhibits a second-order system dynamics.

The tracking performance of the proposed control method is shown in Figs. 3-5. Figure 3a displays the step voltage response of the controller for  $V_d = -5\text{V}$  and  $V_d = -20\text{V}$ . The converter settles less than 1 ms with a negligible overshoot. The tracking error at

steady-state is almost zero, but not zero due to the limited switching frequency of the pulse-width modulators. The inductor currents shown in Fig. 3b varies with  $\bar{I}_1 = V_d^2/RE$ . The average input signal satisfies the operation values given in (2), i.e.,  $u_{ave} = 0.294$  for  $V_d = -5\text{V}$  and  $u_{ave} = 0.625$  for  $V_d = -20\text{V}$  as seen in Fig. 3c. Figure 4 shows the steady state input inductor current which exhibits around 1A ripples compatible to converter design equations given in (11). Again the finite switching frequency causes the current ripples.

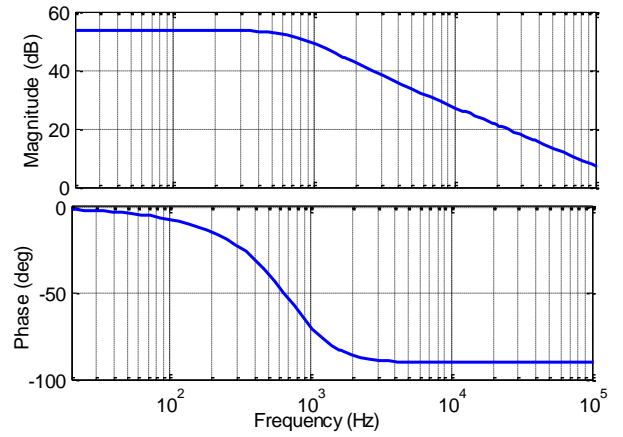


Fig. 2. Frequency response of the controlled Ćuk converter.

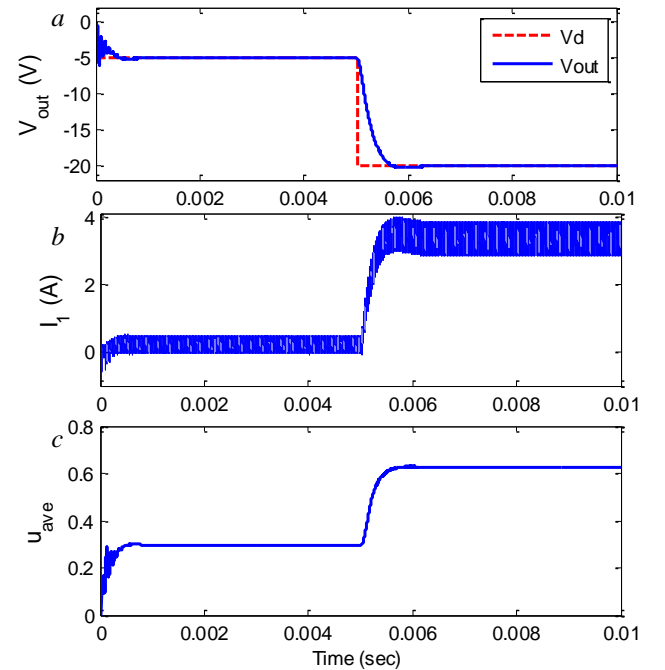


Fig. 3. Numerical simulation results, a) output voltage, b) inductor currents, c) average control signal.

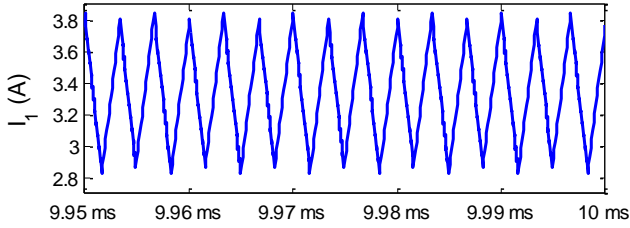


Fig. 4. Steady-state inductor current when  $V_d = -20$  V.

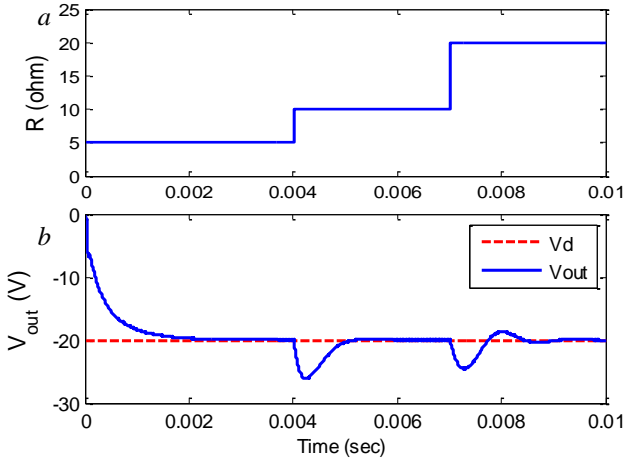


Fig. 5. Numerical tracking performance for step loads, a) load variations,  $5 \leq R(\Omega) \leq 20$ , b) output voltage.

Figure 5 illustrates the robustness performance of the proposed controller. When the load resistance varies in the range of  $5 \leq R(\Omega) \leq 20$ , it is clear that the output voltage tracks the reference signal with zero steady-state error. The numerical results show highly satisfactory robust performance.

### B. Circuit Realization of the Controller

A low cost controller implementation with minimum number of measurements is taken into account. In the design of Ćuk converter elements, the following formulas are used,

$$L_{1,2} = \frac{\bar{u}E}{f_s \Delta L_{L_{1,2}}}, \quad C_1 = \frac{\bar{u}V_o}{Rf_s \Delta V_{C_1}}, \quad C_2 = \frac{\bar{u}E}{8L_2 f_s^2 \Delta V_{C_2}} \quad (11)$$

where  $\Delta L_{1,2}$  and  $\Delta C_{1,2}$  are the inductor and capacitor ripples,  $f_s$  is the switching frequency, and  $V_o$  is the output voltage. The switching frequency is selected as  $f_s = 300$  kHz for the PWM comparator. The converter elements have the values of  $L_1 = L_2 = 22 \mu\text{H}$ ,  $C_1 = 2.2 \mu\text{F}$ ,  $C_2 = 22 \mu\text{F}$ . The supply voltage is  $E = 12$  V, and the resistive load is taken as  $R = 10 \Omega$ . The controller circuit is composed of voltage divider, shunt current sense amplifier, difference amplifiers, integrator and PWM comparator as shown

in Fig. 6. In the integrator design, for a desired transient response, the integrator time constant is taken as  $R_I C_I = 1$  ms with suitable component values, e.g.,  $R_I = 2.2$  k $\Omega$  and  $C_I = 0.47$   $\mu\text{F}$ . It should be noted that in the circuit implementation of controller, a hysteretic comparator is also designed but it would not work during start up without any modification. The switch currents based hysteretic comparator works, but its performance is worse than the PWM based realization because large output ripples are observed.

The performance of the Ćuk converter with the control circuit is provided in Figs. 7-11. The results are given for step-down voltage and step-up voltage references. Figures 7-8 show the circuit results for a step-down voltage reference  $V_d = -5$  V. The start-up response of the controller is seen in Fig. 7, which shows less than 1 ms settling time without any overshoot and practically zero steady-state error. The results are compatible with the numerical results.

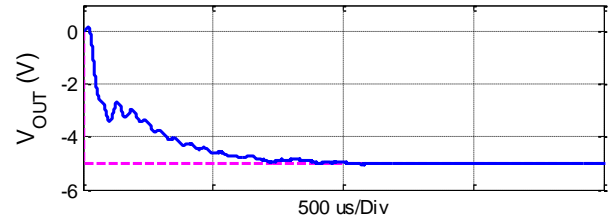


Fig. 6. Circuit tracking performance of the proposed controller for -5V reference signal.

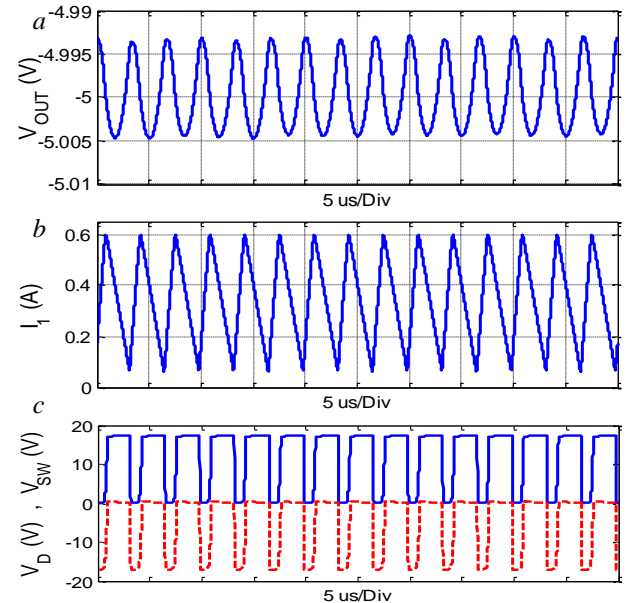


Fig. 7. Steady-state waveforms for  $V_d = -5$  V, a) output voltage, b) inductor current, c) switch voltages.

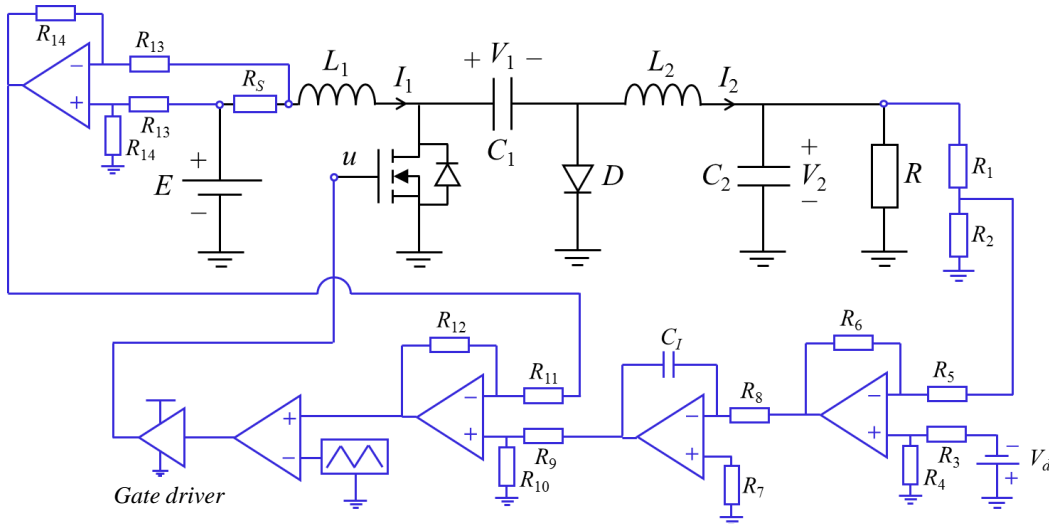


Fig. 8. Circuit realization of the proposed control scheme for the Ćuk converter.

The steady-state values of the output voltage, inductor current and switch waveforms are illustrated in Fig. 8. The output voltage ripple is around  $\Delta V_2 = \bar{u}V_o/(RCf_s) = 0.01 V$  (0.2%) due to the switching frequency as seen in Fig. 8a. The current ripple of the input inductor can be calculated from (11) as  $\Delta I_1 = \bar{u}E/(f_sL_1) = 545 mA$  as observed in Fig. 8b. The current value of the circuit is larger than the numerical values due to the circuit imperfections and parasitic losses. The MOSFET switch and diode works in a complementary fashion as seen in Fig. 8c.

Figures 9-11 display the circuit realization results for a reference signal  $V_d = -20 V$ . Again the converter settles down less than 1 ms with a negligible overshoot. Figure 10a shows voltage fluctuations as  $\Delta V_2 = \bar{u}V_o/(RCf_s) = 0.02 V$  (0.1%) due to the switching frequency. The steady-state inductor current has  $\Delta I_1 = \bar{u}E/(f_sL_1) = 1 A$  current ripple as given in Fig. 10b. Figure 10c displays voltages of the semiconductor switches. The fast Fourier transform based power spectral density (PSD) calculation result is shown in Fig. 11 for converter output voltage ripples. In the PSD calculation, the d.c. component of the output voltage is removed, and the remaining small a.c. signal has periodic fluctuations related to the switching frequency ( $f_s = 300 kHz$ ) and its harmonics. Consequently, the results show that the proposed controller provides a highly satisfactory performance.

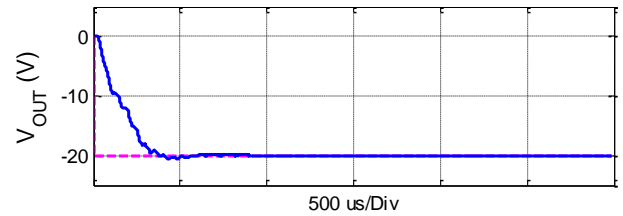


Fig. 9. Circuit tracking performance of the proposed controller for -20 V reference signal.

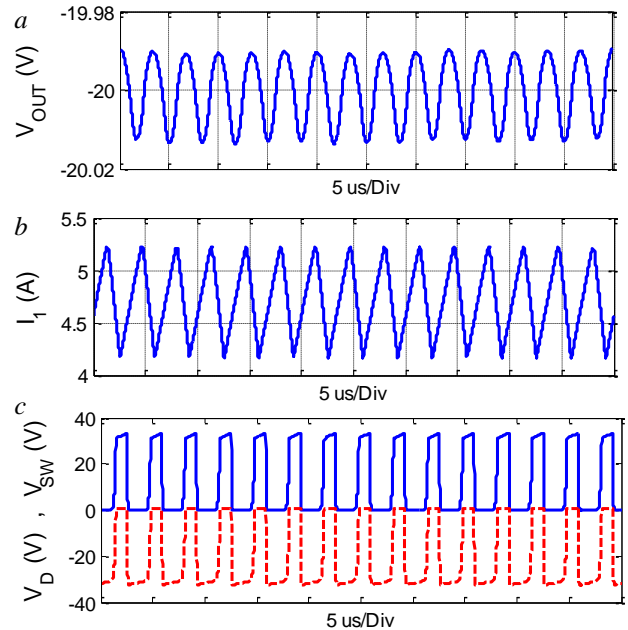


Fig. 10. Steady-state waveforms for  $V_d=-20V$ , a) output voltage, b) inductor current, c) switch voltages.

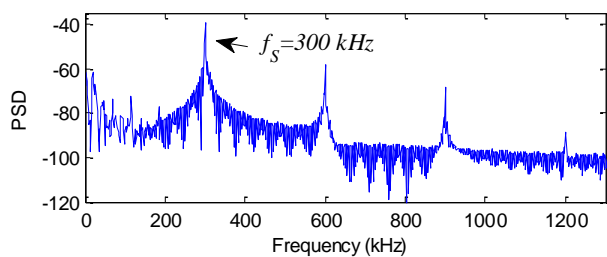


Fig. 11. Power spectral density of output voltage ripples.

#### 4. Conclusion

A robust current feedback based controller is proposed for Cuk converters. The variable structure nature of the converter is utilized for developing a variable structure controller with integral switching manifold. The input inductor current and output voltage feedbacks are used in the controller design. The designed controller has only one control parameter and requires minimum number of circuit elements which ensure low cost and small size for practical implementations. With numerical and circuit realizations, it is shown that the proposed controller provides a fast dynamic response, and practically zero steady-state tracking error. The controller is also robust against load and source variations. The theoretical and practical results are compatible with each other and validate the feasibility of the controller.

#### References

- [1] V. Bist and B. Singh, "A Unity Power Factor Bridgeless Isolated Cuk Converter-Fed Brushless DC Motor Drive," *IEEE Trans. Ind. Electron.*, vol. 62, no. 7, pp. 4118–4129, Jul. 2015.
- [2] J. Qi and D. D. C. Lu, "A Preventive Approach for Solving Battery Imbalance Issue by Using a Bidirectional Multiple-Input Cuk Converter Working in DCVM," *IEEE Trans. Ind. Electron.*, vol. PP, no. 99, pp. 1–1, 2017.
- [3] S. Singh and B. Singh, "A Voltage-Controlled PFC Cuk Converter-Based PMBLDCM Drive for Air-Conditioners," *IEEE Trans. Ind. Appl.*, vol. 48, no. 2, pp. 832–838, Mar. 2012.
- [4] A. R. Saxena, A. Kulshreshtha, and P. Bansal, "Universal bus digitally controlled front end damped PFC Cuk converter as LED drivers," in *IEEE 1st International Conference on Power Electronics, Intelligent Control and Energy Systems (ICPEICES)*, 2016, pp. 1–6.
- [5] W. Chen, Y. Liu, X. Li, T. Shi, and C. Xia, "A Novel Method of Reducing Commutation Torque Ripple for Brushless DC Motor Based on Cuk Converter," *IEEE Trans. Power Electron.*, vol. 32, no. 7, pp. 5497–5508, 2017.
- [6] D. G. Lamar, J. S. Zuniga, A. R. Alonso, M. R. Gonzalez, and M. M. H. Alvarez, "A Very Simple Control Strategy for Power Factor Correctors Driving High-Brightness LEDs," *IEEE Trans. Power Electron.*, vol. 24, no. 8, pp. 2032–2042, Aug. 2009.
- [7] K. M. Smedley and S. Cuk, "One-cycle control of switching converters," *IEEE Trans. Power Electron.*, vol. 10, no. 6, pp. 625–633, Nov. 1995.
- [8] J. L. Flores, J. L. B. Avalos, and C. A. B. Espinosa, "Passivity-Based Controller and Online Algebraic Estimation of the Load Parameter of the DC-to-DC power converter Cuk Type," *IEEE Lat. Am. Trans.*, vol. 9, no. 1, pp. 784–791, Mar. 2011.
- [9] J. Neely, R. DeCarlo, and S. Pekarek, "Real-time model predictive control of the Cuk converter," in *12th Workshop on Control and Modeling for Power Electronics (COMPEL)*, 2010, pp. 1–8.
- [10] L. Cavanini, G. Cimini, and G. Ippoliti, "Model predictive control for the reference regulation of current mode controlled DC-DC converters," in *14th International Conference on Industrial Informatics (INDIN)*, 2016, pp. 74–79.
- [11] A. Balestrino, A. Landi, and L. Sani, "Cuk converter global control via fuzzy logic and scaling factors," *IEEE Trans. Ind. Appl.*, vol. 38, no. 2, pp. 406–413, Mar. 2002.
- [12] J. Mahdavi, M. R. Nasiri, A. Agah, and A. Emadi, "Application of neural networks and State-space averaging to DC/DC PWM converters in sliding-mode operation," *IEEEASME Trans. Mechatron.*, vol. 10, no. 1, pp. 60–67, Feb. 2005.
- [13] A. H. Zaeri, M. B. Poodeh, and S. Eshtehardiha, "Improvement of Cuk converter performance with optimum LQR controller based on genetic algorithm," in *International Conference on Intelligent and Advanced Systems*, 2007, pp. 917–922.
- [14] A. Kugi and K. Schlacher, "Nonlinear H infinity controller design for a DC-to-DC power converter," *IEEE Trans. Control Syst. Technol.*, vol. 7, no. 2, pp. 230–237, Mar. 1999.
- [15] S. Buso, G. Spiazzi, and D. Tagliavia, "Simplified control technique for high-power-factor flyback Cuk and Sepic rectifiers operating in CCM," *IEEE Trans. Ind. Appl.*, vol. 36, no. 5, pp. 1413–1418, Sep. 2000.
- [16] E. A. Aksenov and V. D. Yurkevich, "Control system design based on sliding mode control and singular perturbation technique for a Cuk converter," in *13th International Scientific-Technical Conference on Actual Problems of Electronics Instrument Engineering (APEIE)*, 2016, vol. 03, pp. 77–82.
- [17] F. Ahmad, A. Rasool, E. Ozsoy, A. Sabanovic, and M. Elitas, "Design of a robust cascaded controller for Cuk converter," in *IEEE International Power Electronics and Motion Control Conference (PEMC)*, 2016, pp. 80–85.
- [18] P. Deivasundari, G. Uma, and S. Ashita, "Chaotic dynamics of a zero average dynamics controlled DC-DC Cuk converter," *IET Power Electron.*, vol. 7, no. 2, pp. 289–298, Feb. 2014.
- [19] J. Knight, S. Shirsavar, and W. Holderbaum, "An improved reliability cuk based solar inverter with sliding mode control," *IEEE Trans. Power Electron.*, vol. 21, no. 4, pp. 1107–1115, Jul. 2006.
- [20] Z. Chen, "PI and Sliding Mode Control of a Cuk Converter," *IEEE Trans. Power Electron.*, vol. 27, no. 8, pp. 3695–3703, Aug. 2012.
- [21] S. C. Tan and Y. M. Lai, "Constant-frequency reduced-state sliding mode current controller for Cuk converters," *IET Power Electron.*, vol. 1, no. 4, pp. 466–477, Dec. 2008.